Science & Technology Development Journal 2023, 26(3):2975-2986

Open Access Full Text Article

Engineering & Technology: Research Article

Improving the performance of the GPS/INS integrated navigation system by using the real-time kinematic method

Dung Quoc Tien Tran[1,2,*], Vinh Hao Nguyen[1,2]

ABSTRACT

Introduction: This paper presents a method for improving the accuracy of a GPS/INS integrated navigation system. Estimating the yaw angle, which is the degree of deviation from the north, is a crucial aspect in the navigation and control of autonomous robots. **Methods**: We can use an inertial measurement unit (IMU) to calculate the yaw angle, but the accuracy is heavily reliant on the Earth's magnetic field. This field can vary in value as the vehicle moves and is easily disturbed by external sources such as electrical devices and motors. To circumvent these limitations, a dual-antenna GPS with the real-time kinematic (RTK) method is utilized to improve the quality of the yaw angle estimation. **Results**: This approach eliminates the use of magnetometers, and the experimental results show that the error can be significantly reduced to 0.16 degrees with a baseline of 1 meter. **Conclusion**: When compared to the standard GPS/INS system, the proposed method using GPS-RTK provides better accuracy, even when the GPS signal is lost.

Key words: Inertial Navigation System, Global Positioning System, Integrated Navigation System, Real-time Kinematic

[1]*Department of Control Engineering and Automation, Faculty of Electrical and Electronics Engineering, Ho Chi Minh City University of Technology, 268 Ly Thuong Kiet Street, District 10, Ho Chi Minh City, Vietnam*

[2]*Vietnam National University Ho Chi Minh City (VNUHCM), Linh Trung Ward, Ho Chi Minh City, Vietnam*

Correspondence

Dung Quoc Tien Tran, Department of Control Engineering and Automation, Faculty of Electrical and Electronics Engineering, Ho Chi Minh City University of Technology, 268 Ly Thuong Kiet Street, District 10, Ho Chi Minh City, Vietnam

Vietnam National University Ho Chi Minh City (VNUHCM), Linh Trung Ward, Ho Chi Minh City, Vietnam

Email: tqtiendung@hcmut.edu.vn

History

- Received: 2023-07-09
- Accepted: 2023-08-10
- Published Online: 2023-9-30

DOI :

https://doi.org/10.32508/stdj.v26i3.4120

INTRODUCTION

Navigation systems play a crucial role in guiding and controlling autonomous robots. Its accuracy affects the quality of control. There are currently multiple methods to determine the position, velocity, and attitude of a vehicle in a global or local coordinate system, such as dead-reckoning, landmark-based positioning, and map-based positioning. Dead-reckoning systems use inertial measurements to estimate the robot's displacement since the last sampling epoch. Landmark-based positioning involves sensors that measure the distance and angle between the robot and predefined landmarks, from which calculations are performed to determine the vehicle's position. Map-based positioning uses distance sensors to detect environmental boundaries and then compares them to a prestored map to determine the robot's position on the map. Each method has its advantages and disadvantages. For example, dead-reckoning provides highly accurate results in a short amount of time but accumulates errors over time, especially when using low-cost sensors [1].

Currently, the common practice is to combine diverse positioning techniques to maximize their advantages. One approach is to integrate inertial navigation systems (INS) and global navigation systems (GPS) to create a highly accurate and robust system. However, using low-cost sensors such as MEMS-based IMUs can result in high biases, requiring accurate sensor calibration techniques [2]. GPS systems may also experience signal interruptions due to obstruction by tall buildings, mountains, or forests. The authors in [3–5] have worked on improving INS/GPS integration and calibration methods, such as reducing sensor drift and using raw GPS measurements, including pseudorange and Doppler measurements, to estimate continuous positions even with fewer than four satellite signals. At present, with the rapid development of artificial intelligence, the application of neural network models to GPS/INS navigation systems is also being widely studied [6]. The authors in [7] and [8] introduce GPS/INS neural network frameworks that can help reduce errors in the case of GPS outages. However, the studies have been limited to the level of offline data collection and processing by computers and have not yet been applied to hardware using microcontrollers.

Real-time kinematic (RTK) is a method to improve GPS positioning accuracy using raw measurements (carrier phase measurement). According to [9], the results obtained from standalone GPS receivers are often affected by atmospheric disturbances, multipath errors, and time synchronization errors between the satellites and receivers. The authors suggest that using the single-difference method can eliminate biases between receivers or satellites, and using the double-difference method can eliminate biases between receivers and satellites. In [10], Consoli et al. proposed

Cite this article : Tran D Q T, Nguyen V H. **Improving the performance of the GPS/INS integrated navigation system by using the real-time kinematic method** . *Sci. Tech. Dev. J.* 2023; 26(3):2975-2986.

the idea of using multiple GPS receivers to determine the yaw angle, but the paper only focused on the concept and simulated the impact of changing baselines (the distance between antennas). Papers [11] and [12] introduced models using multiple GPS receivers to determine the yaw angle and compared the simulation results. In [13], the authors combined a highly accurate IMU and two GPS receivers (one high-precision and one low-cost) to build an integrated positioning system with an accuracy of 0.2 degrees for the yaw angle with a baseline of 92 centimeters. However, this system has a high total cost.

In this paper, the authors introduce a new GPS/INS integration method, which uses yaw measurement from a dual-antenna GPS to enhance the positioning quality. For the dual-antenna GPS, experiments are conducted to investigate the relationship between the angle estimation quality and the baseline distance, as well as the influence of the number of GPS carrier frequencies used in the system. The hardware of the GPS/INS system is also fully built. The results show that the use of additional angle estimators results in better positioning quality than traditional GPS/INS systems when there is a GPS outage. Following the introduction, there are 3 sections in this paper. Section 2 presents the theoretical basis of the dual-antenna GPS and improvements in the GPS/INS system. Section 3 introduces the hardware models used in the experiments, along with the experimental results and comments. The conclusions and future works are given in the last section.

METHODS

Yaw angle estimation using dual-antenna GPS

Figure 1 describes how the GPS-RTK method works. In this method, base station (b) is stationary and has a previously known position. The rover station (r) is the moving station and is usually attached to the vehicles that need to be located. The GPS-RTK system uses the carrier phase offset (denoted as f) between the satellites and the stations to determine the exact position of the rover. This method can achieve a centimeter-level position [10]. However, in determining the yaw angle based on GPS, both the base and rover antennas are mounted on moving vehicles. To determine the position of the base station, the single-point positioning method is used. This method uses pseudorange measurements to calculate position based on the least squared error technique and can achieve an accuracy of approximately 2 meters to 5 meters. After that, the RTK algorithm is used to determine the position of the rover, and this method is called moving-base RTK. This method only focuses on the relative position between the two antennas, and the accuracy of the position is not high due to the single-point positioning method used to determine the position of the base station. Another method proposed in [14] is that the GPS-RTK algorithm can use pseudorange measurements and an extended Kalman filter to determine the approximate positions of both the base and rover and then use phase measurements to calculate the results with high accuracy.

Figure 2 describes a flowchart of the GPS-RTK algorithm. There are 3 important steps that need to be noted, which have been numbered 1, 2, and 3 in the figure. First, the GPS receiver at the rover station uses the single-point positioning method to determine its position with low accuracy. Since the algorithm uses the first-order and second-order differentials of the carrier phase measurements, it is necessary to determine the satellites that are "seen" by both the base and rover receivers. If the number of common satellites is less than 4, the RTK algorithm cannot be applied. On the other hand, by combining the measurements with the Extended Kalman Filter (EKF), we obtain the position of the rover with an accuracy of approximately 1 meter. This method is also known as DGPS (step 1). In step 2, we find the solution to the integer ambiguities problem. This is an integer optimization problem and can be solved using the LAMBDA or MLAMBDA algorithm [15]. If we find the solution to the problem, we can find the position of the rover station with an accuracy of up to centimeters (step 3). At the same time, we can calculate the yaw angle based on the relative position of the two objects in the Earth-centered, Earth-fixed (ECEF) coordinate system. Article [14] describes in detail the formulas used for the GPS/RTK algorithm.

The GPS/INS integrated navigation system

Based on the complexity of integration between GPS and INS systems, considering factors such as interaction, independence, and the amount of shared information between the two systems, we can categorize the integration methods as follows [1]:

- Uncoupled
- Loosely Coupled (LC)
- Tightly Coupled (TC)
- Deeply Integrated

In the uncoupled method, the two systems operate almost independently. When there is a GPS position update, the positioning results are used to "reset" the INS. Conversely, when GPS is disrupted, the

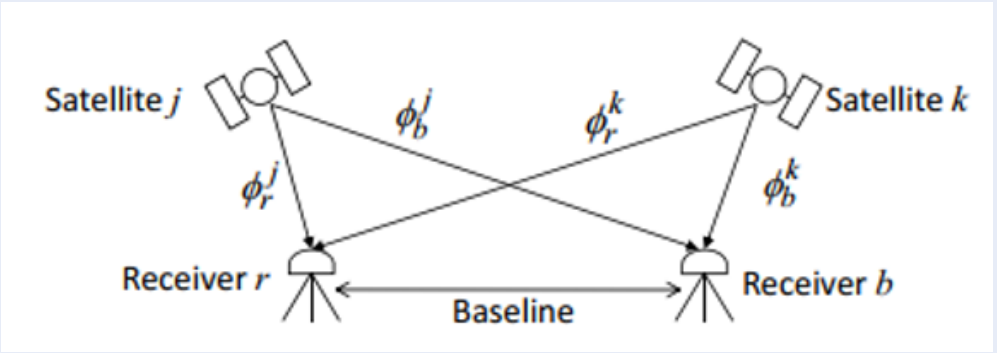

Figure 1: **A visualization of the GPS-RTK algorithm.**

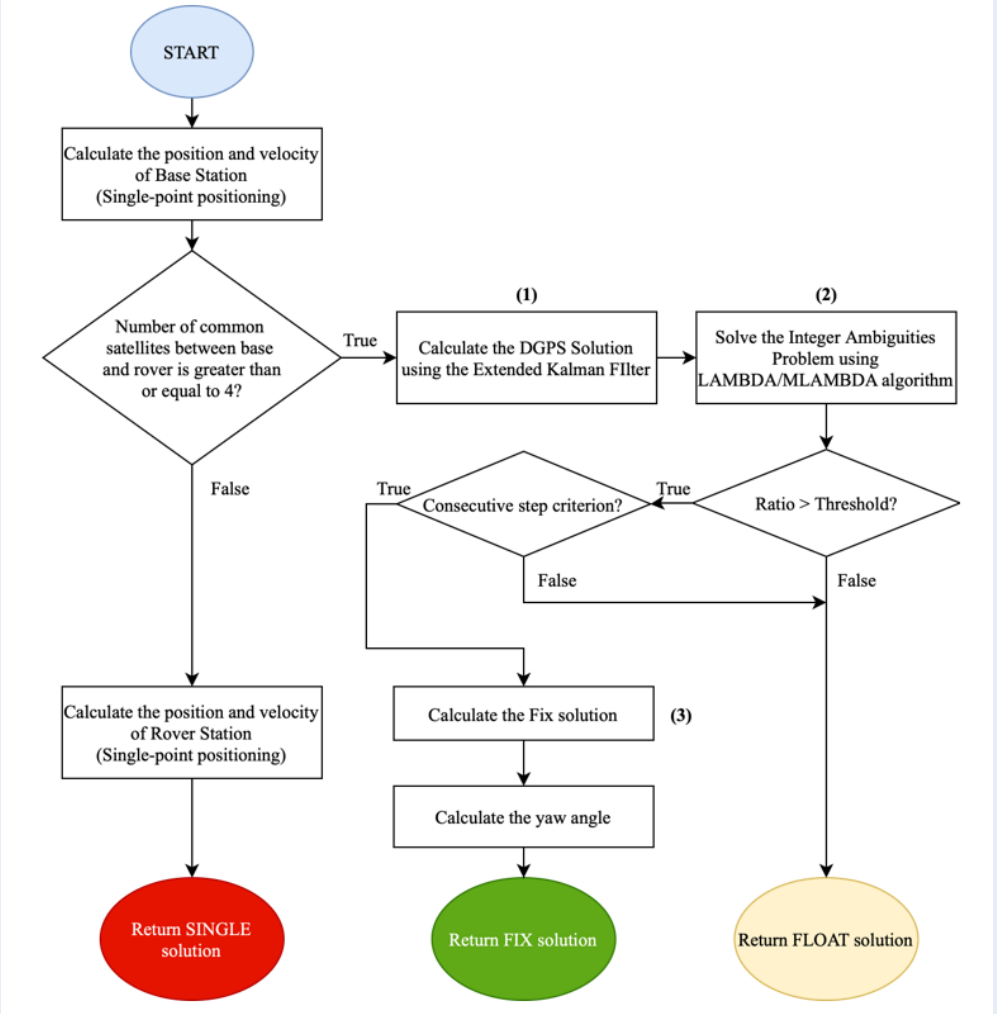

Figure 2: **Flowchart of the GPS-RTK algorithm**.

dead-reckoning estimation from the INS is used. This method is the simplest in structure, but the system cannot estimate the bias drift of the sensors. Due to this drawback, despite its simplicity, this method is not widely used.

The LC, also known as the "decentralized" structure, includes a nonlinear estimator to combine the INS estimation results with the position and velocity results of the GPS and another filter to determine the position and velocity from raw GPS results, such as pseudorange and Doppler measurements. Figure 3 illustrates its diagram.

The inertial navigation system (INS) uses the position (longitude λ, latitude φ and altitude h), velocity values (v_N for the north, v_E for the east, and v_D for the vertical down direction), and attitude (roll ϕ, pitch θ, yaw ψ, which represent rotations around the x, y, and z axes, respectively) of the previous sampling epoch, combined with inertial measurements (tri-axial angular rate $\omega_{x,y,z}$ and acceleration $f_{x,y,z}$ along with calibration parameters for Earth model deviations, to estimate the system's state at the current epoch.

Referring to [3], we have the equations of the INS mechanization system:

$$\frac{d}{dt}C_b^n = C_b^n.\Omega_{ib}^b - \Omega_{ie}^n - \Omega_{en}^n \tag{1}$$

The symbol C_b^n denotes a direction cosine matrix (DCM), calculated from the Euler angles roll, pitch, and yaw by equation (2). Ω is the skew-symmetric matrix of the angular velocity vector ω. ω_{ib}^b is the angular rate measured from the gyroscopes. ω_{ie}^n and ω_{en}^n are the bias correction vectors due to the Coriolis effect. The magnitude of the Coriolis-induced angular velocity depends on the geographic location of the vehicle.

$$C_b^n = \begin{bmatrix} C_\theta C_\psi & -C_\phi S_\psi + S_\phi S_\theta S_\psi & C_\phi C_\psi + S_\phi S_\theta S_\psi \\ C_\theta S_\psi & S_\phi S_\psi + C_\phi S_\theta C_\psi & -S_\phi C_\psi + C_\phi S_\theta S_\psi \\ -S_\theta & S_\phi C_\theta & C_\phi C_\theta \end{bmatrix} \tag{2}$$

The next step in the process of INS mechanization is velocity update:

$$\frac{d}{dt}v = f + g - (2\Omega_{ie}^n + \Omega_{en}^n).v \tag{3}$$

In the above equation, f is the measured acceleration and g is the gravity vector. In this paper, gravity is chosen as a vector pointing to the center of the Earth, whose magnitude is constant at 9.80665 m.s-2. In reality, it depends on the geographic location, but this model is complex, and the value does not vary much, so it can be ignored [4]. Similarly, we have equations to update the position:

$$\dot{r} = \begin{bmatrix} \dot{\varphi} \\ \dot{\lambda} \\ \dot{h} \end{bmatrix} = \begin{bmatrix} \frac{1}{M+h} & 0 & 0 \\ 0 & \frac{1}{(N+h)\cos(\varphi)} & 0 \\ 0 & 0 & -1 \end{bmatrix} v \tag{4}$$

where M and N are the radii of curvature of the meridian and prime vertical passing through the vehicle, respectively. Their values depend only on the current latitude of the vehicle. In practical calculations, due to the limited computational capabilities, equations (1), (3), and (4) are used in discrete form. This is typically done through the use of numerical integration methods, such as the Runge–Kutta method.

The loosely coupled model is based on the extended Kalman filter, where the state vector includes 15 components divided into 5 groups as follows: position error δr, velocity error δv, rotation matrix error ε, accelerometer bias δb_a, and gyroscope bias δb_g. Each group has 3 values that correspond to 3 axes. The modeling of the position, velocity, and orientation errors is calculated by taking derivatives of the equations mentioned above. The IMU sensor errors consist of two components: fixed bias and bias drift. Based on calibrations in the laboratory, the fixed bias component can be compensated. However, the bias drift component does not repeat in each experiment, so it must be a concern in the system. The random drift error can be modeled using the Gauss–Markov model [16] as follows:

$$\frac{d}{dt}\delta b_{a,i} = -\frac{1}{\tau_{ba,i}}\delta b_{a,i} + \eta_{ba,i} \tag{5}$$

$$\frac{d}{dt}\delta b_{g,i} = -\frac{1}{\tau_{bg,i}}\delta b_{g,i} + \eta_{bg,i} \tag{6}$$

where the letter i represents the x, y, and z axes. Denote τ as the correlation time and η as the variance of white noise according to the Gauss–Markov model. The correlation time and variance of the noise can be obtained using the correlation analysis method [4]. The method used in this paper is the Allan variance analysis.

Finally, we have the process model of the Extended Kalman Filter for the GPS/INS TC model in equation (7), where S(k) is the skew-symmetric matrix of the vector k. Regarding the measurement model, we have 6 measurements of position (latitude, longitude, and altitude) and velocity (north, east, down) from the GPS. These values are compared with the estimated

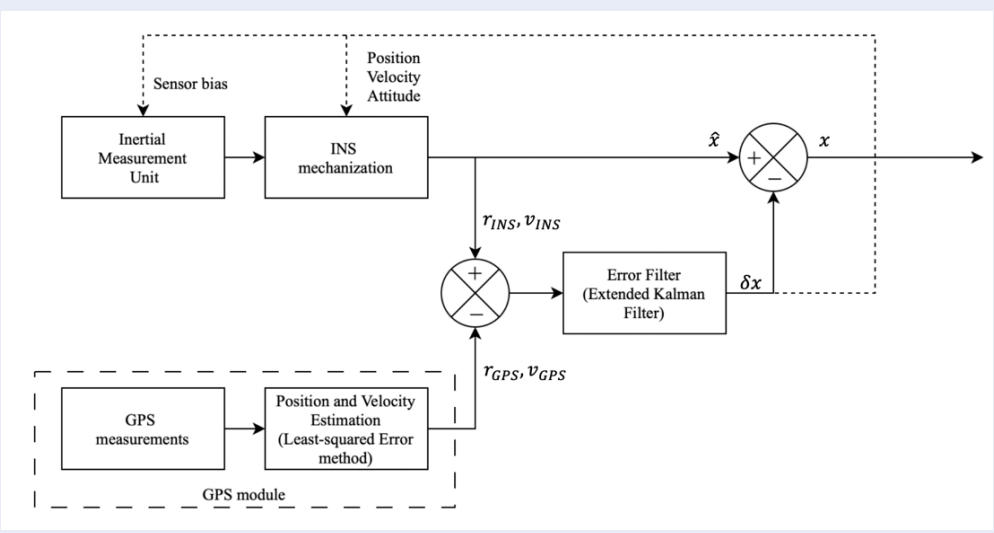

Figure 3: **Structure of the LC GPS/INS system**.

position and velocity from the INS to estimate the bias drift of the IMU sensor.

$$\frac{d}{dt}\begin{bmatrix}\delta r\\ \delta v\\ \varepsilon\\ \delta b_a\\ \delta b_g\end{bmatrix}=\begin{bmatrix}\delta r\\ \delta v\\ \varepsilon\\ \delta b_a\\ \delta b_g\end{bmatrix}\times \begin{bmatrix}F_{rr} & F_{rv} & 0_{3x3} & 0_{3x3} & 0_{3x3}\\ F_{vr} & F_{vv} & S(f) & C_b^n & 0_{3x3}\\ F_{er} & F_{ev} & -S(\omega_{in}^n) & 0_{3x3} & -C_b^n\\ 0_{3x3} & 0_{3x3} & 0_{3x3} & -1/\tau_{ba} & 0_{3x3}\\ 0_{3x3} & 0_{3x3} & 0_{3x3} & 0_{3x3} & -1/\tau_{bg}\end{bmatrix} + \begin{bmatrix}0_{3x3} & 0_{3x3} & 0_{3x3} & 0_{3x3}\\ C_b^n & 0_{3x3} & 0_{3x3} & 0_{3x3}\\ 0_{3x3} & -C_b^n & 0_{3x3} & 0_{3x3}\\ 0_{3x3} & 0_{3x3} & I_3 & 0_{3x3}\\ 0_{3x3} & 0_{3x3} & 0_{3x3} & I_3\end{bmatrix}\begin{bmatrix}\eta_a\\ \eta_g\\ \eta_{ba}\\ \eta_{ba}\end{bmatrix} \quad (7)$$

A modification to apply yaw angle estimation from GPS moving-base RTK

Figure 4 describes an advanced GPS/INS integrated navigation system using the LC method with yaw angle measurements from a dual-antenna GPS. Compared to Figure 3, it can be seen that the original model was further improved in the GPS subsystem. We expand the single GPS with 6 measurements (3 positions and 3 velocities) to a dual-antenna GPS with 7 measurements (adding yaw angle measurement). In the vanilla GPS/INS system, the attitude error vector ε is the error of the direction cosine matrix C_b^n. Considering the relationship between the error of the rotation matrix and the attitude errors (roll, pitch, yaw) errors, denoted by $\delta\phi$,$\delta\theta$, and $\delta\psi$, respectively, we have 2 methods of error calculation:

$$\widehat{C}_b^n=\left(I_3-\begin{bmatrix}0 & -\varepsilon_D & \varepsilon_E\\ \varepsilon_D & 0 & -\varepsilon_N\\ -\varepsilon_E & \varepsilon_N & 0\end{bmatrix}\right)C_b^n \quad (8)$$

$$\widehat{C}_b^n=C_b^n+R_1R_2\frac{\partial R_3}{\partial\phi}\delta\phi +R_1R_3\frac{\partial R_2}{\partial\theta}\delta\theta+R_2R_3\frac{\partial R_1}{\partial\psi}\delta\psi \quad (9)$$

where R1, R2, and R3 are the rotation matrices for yaw, pitch, and roll about the z, y, and x axes, respectively. Therefore, the transformation between the two types of attitude errors, ε and $\begin{bmatrix}\delta\phi & \delta\theta & \delta\psi\end{bmatrix}^T$, is extremely complex. To incorporate the yaw error measurements from the GPS-RTK system into the GPS/INS system, we need to transform the process model equation (7).

We use a new state vector x= $\begin{bmatrix}\delta r & \delta v & \delta a & \delta b_a & \delta b_g\end{bmatrix}^T$, where δ_a= $[\delta\phi\ \delta\theta\ \delta\psi]^T$ is the attitude error vector of the Euler angles. By performing the Taylor series expansion and taking the first-order derivative in the same way as in Section 2.2, we have the following updated equations for position and velocity:

$$\frac{d}{dt}\delta r=F_{rr}\delta r+F_{rv}\delta v \quad (10)$$

$$\frac{d}{dt}\delta v=F_{vr}\delta r+F_{vv}\delta v+R_1R_2\frac{\partial R_3}{\partial\phi}\delta\phi +R_1R_3\frac{\partial R_2}{\partial\theta}\delta\theta+R_2R_3\frac{\partial R_1}{\partial\psi}\delta\psi+C_b^n\delta b_a \quad (11)$$

We can see that the equation of position error (11) is identical to the original model presented in (7), as the

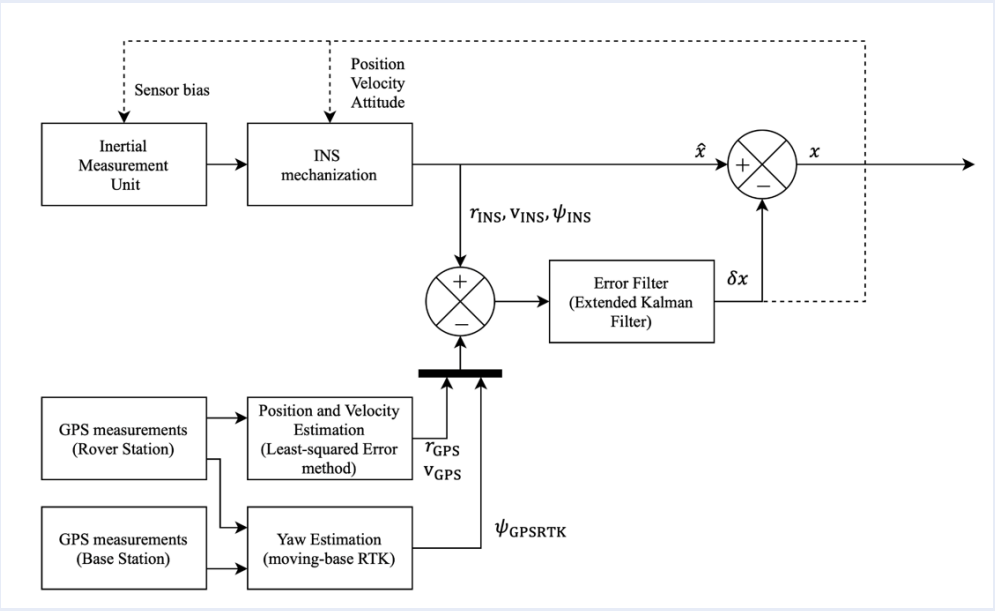

Figure 4: **Diagram of the GPS/INS LC model with yaw estimation from GPS-RTK .**

position update is not dependent on attitude. However, there is a slight modification in the equation for velocity error, from S(f).ε to F_{va}.δa. The matrix F_{va} is defined as:

$$F_{va} = \begin{bmatrix} R_1R_2\dfrac{\partial R_3}{\partial \phi} & 0 & 0 \\ 0 & R_1R_3\dfrac{\partial R_2}{\partial \theta} & 0 \\ 0 & 0 & R_1R_2\dfrac{\partial R_1}{\partial \psi} \end{bmatrix} \quad (12)$$

Regarding the formula for updating the angle, the calculations are quite lengthy, so this paper only mentions the final formula in the form of:

$$\frac{d}{dt}\delta a = F_{ar}\delta r + F_{av}\delta v + F_{aa}\delta a + F_{abg}\delta b_g \quad (13)$$

$$F_{abg} = \begin{bmatrix} 1 & \sin(\phi)\tan(\theta) & \cos(\phi)\tan(\theta) \\ 0 & \cos(\phi) & -\sin(\phi) \\ 0 & \sin(\phi)sec(\theta) & \cos(\phi)sec(\theta) \end{bmatrix} \quad (14)$$

$$F_{ar} = -F_{abg}.\left(C_b^n\right)^T.F_{er} \quad (15)$$

$$F_{av} = -F_{abg}.\left(C_b^n\right)^T.F_{ev} \quad (16)$$

$$F_{aa} = \left[F_{a\phi}\ F_{a\theta}\ F_{a\psi}\right] \quad (17)$$

$$F_{a\phi} = \frac{\partial F_{abg}}{\partial \phi}.\omega_{nb}^b - F_{abg}\left[R_1R_2\frac{\partial R_3}{\partial \phi}\right]^T\omega_{in}^n \quad (18)$$

$$F_{a\theta} = \frac{\partial F_{abg}}{\partial \theta}.\omega_{nb}^b - F_{abg}\left[R_1R_3\frac{\partial R_2}{\partial \theta}\right]^T\omega_{in}^n \quad (19)$$

$$F_{a\phi} = -F_{abg}\left[R_2R_3\frac{\partial R_1}{\partial \psi}\right]^T\omega_{in}^n \quad (20)$$

We have the definition of trigonometric function-sec(x)=1/cos(x).

RESULTS AND DISCUSSIONS

Hardware implementation

Figure 5 shows the authors' implemented GPS/INS integrated navigation system. The first concern in developing hardware for our system is the processing speed of the microcontroller. We use the STM32H7 microcontroller by STMicroelectronics with a high clock frequency of up to 480 MHz. However, due to the large computational load of both systems, where the GPS with two antennas takes a long time to solve the LAMBDA/MLAMBDA algorithm and the INS requires a high update rate (at least 100 Hz), it is not feasible to use a single-core microprocessor. To solve this problem, we implemented two identical circuits, one for the GPS/INS system and the other for the GPS-RTK system. The developed system has high flexibility, meaning that each system can be reused for different applications. Furthermore, based on the necessary peripheral configuration, we can see that only one PCB design needs to be used for both requirements (Figure 6).

The GPS receivers chosen must have the function of transmitting raw measurements. The receivers are not required to be the same, but it is recommended to use the same type of receiver for both the base and rover in experiments to eliminate the common error between receivers (such as clock bias and clock drift). In this paper, the NEO-M8 GPS receiver (Figure 7a) from Ublox AG[17] is used for the case of using

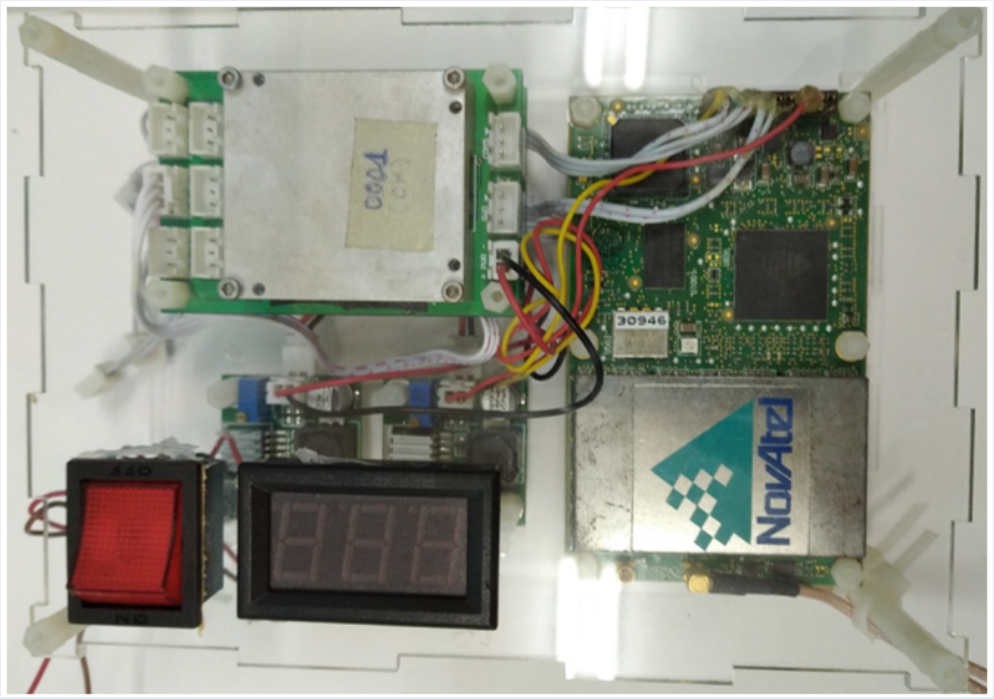

Figure 5: **The implemented GPS/INS integrated navigation system**.

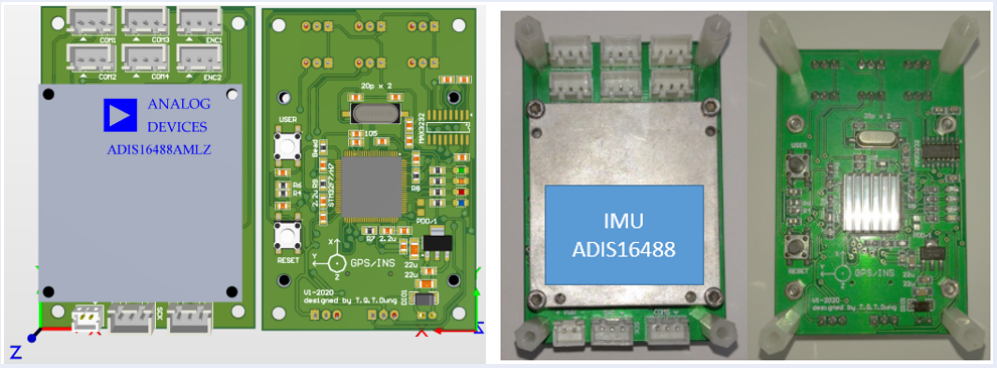

Figure 6: **PCB design of the integrated navigation system**.

a single-frequency carrier wave (L1), with a position accuracy of 2.123 cm + 1 ppm in the case of achieving RTK Fix. In the case of using dual-frequency (L1 and L2) GPS receivers, NovAtel OEMV-2 GPS receivers [18] (Figure 7b) are used. These receivers have a position accuracy of 1 cm + 1 ppm for the RTK fix solution.

Experimental results of the GPS-RTK system

In this experiment, the antennas were placed in a static state. Two antennas were placed at distances of 0.3, 0.5, 1, and 2 meters apart. From the estimated results, we determined the RMS error of the measurement. Then, the least squares method was used to estimate the relationship between the RMS error and the baseline distance. In addition, it was used to compare the quality between the GPS-RTK system using a dual-frequency receiver and a similar system using a single-frequency receiver. The results are shown in Figure 8.

From the above figure, we can see that using a dual-frequency system yields significantly better results compared to using a single-frequency system. The average Fix solution ratio is 69% compared to 60%. In

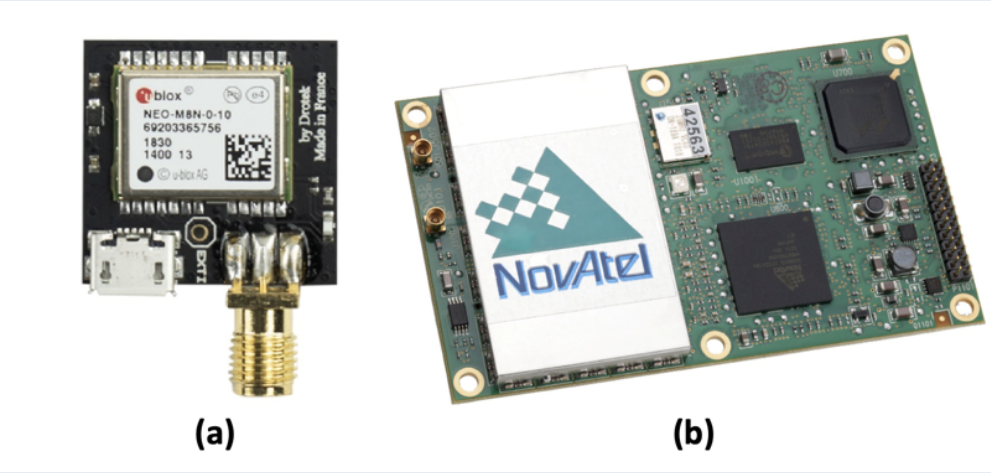

Figure 7: **The GPS receivers used in the experiment.**

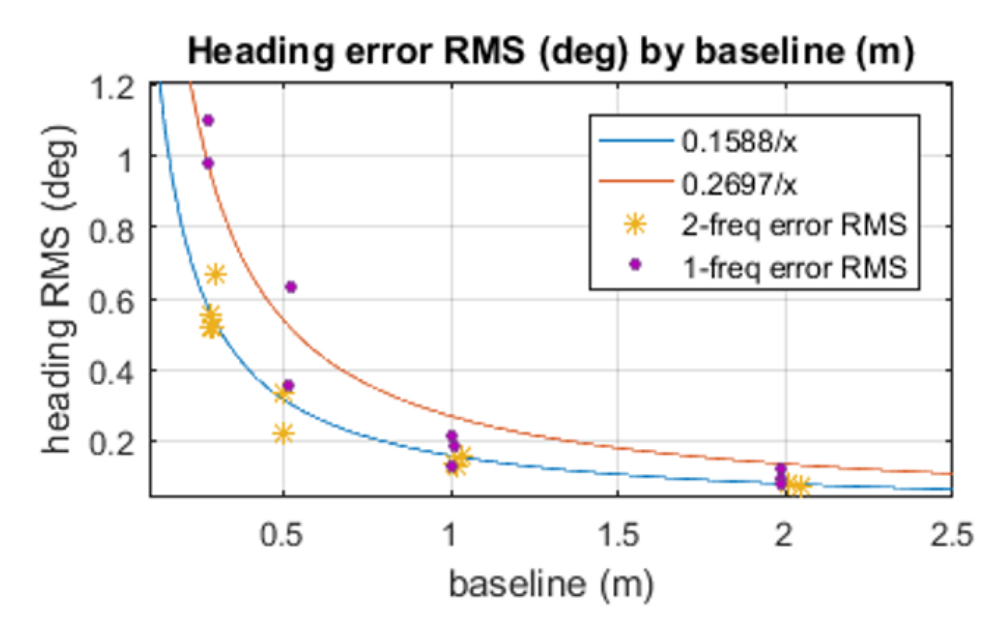

Figure 8: **The relation between the yaw angle RMS error and the baseline length.**

some cases, the single-frequency system cannot find any Fix solution (2 out of 12 datasets). For the yaw error, both types of systems yielded small RMS errors when increasing the baseline length. Theoretical analysis shows that as the distance between the two antennas increases, the yaw error decreases. Comparing the two types of GPS receivers, we see that with the same baseline length, the dual-frequency receiver produces smaller errors than the single-frequency receiver. Examining the technical specifications, the accuracy of the dual-frequency receiver used in the experiment is 1 cm + 1 ppm, which is better than the accuracy of the single-frequency receiver, which is 2.123 cm + 1 ppm. This is why the dual-frequency system yields smaller estimation errors with the same baseline length. If the baseline length increases, the accuracy will improve accordingly. However, autonomous vehicles usually have size limitations, so sometimes it is not feasible to choose a large baseline length.

Experimental results of the modified GPS/INS system with dual-antenna GPS-RTK

First, we consider the case of estimating the bias of the IMU sensor. Typically, the bias drift of the sensor changes slowly, and we set a fixed bias to the sensor to investigate the ability to estimate and compensate for these input values. For comparison, we only consider the case where the system is stationary. The estimated bias values of the GPS/INS system are compared with an Euler angle estimator from the IMU. At this point, the Euler angle estimator is capable of estimating bias and compensating for the external acceleration affecting the IMU. The results are shown in Figure 9 and Figure 10.

We can see that the GPS/INS system can estimate the bias values of the sensors. In the figures, we observe that the sensor estimation response is slow, which is due to the sudden input of bias values that do not fit well with the true bias model. In reality, the bias drift is slower.

Next, we will compare the performance of the GPS/INS integrated navigation system in two cases of yaw angle estimation (using dual-antenna GPS and using a magnetometer). The remaining conditions (roll and pitch angles of the estimation system, using velocity constraints, etc.) are kept the same. In the experimental conditions, the firmware of the positioning system is programmed to simulate GPS signal loss. This means that although the GPS signal remains available, the positioning system will not use it. This function is activated to investigate the stability of the system in cases where the GPS signal is disrupted. This experiment will consider three scenarios of disruption: disruption on a straight road, disruption when making a 90-degree turn, and disruption when making a 180-degree turn (Figure 11 and Figure 12).

In Figure 11, the GPS points used by the GPS/INS system are marked in red, and the GPS points lost are marked in purple. We can see that when the GPS signal is present, the system performs well. The deviation between the GPS/INS and GPS signal is stable at less than 2 m. However, when the GPS signal is lost, the estimated values do not follow the standard trajectory. Figure 12 shows the error-time graph of both methods. The blue and orange lines indicate the errors of the proposed method and original method, respectively. Markers '+', 'o', and 'x' represent the errors when the vehicle is moving on a straight line, making a 90-degree turn, and making a 180-degree turn, respectively. From the graph, we observe that the longest time for maintaining a GPS signal when it is lost is in the case of driving on a straight road (less than 3 meters after 15 seconds). In the case of moving on a curved path, the estimated values tend to increase rapidly. When the GPS signal is lost, the magnetometer-based system is more prone to divergence, even in the case of driving on a straight road. Compared to the dual-antenna GPS-based system, we can see that when the GPS signal is present, both systems are stable. However, when the GPS signal is lost, the dual-antenna GPS-based system is better at maintaining the deviation than using the magnetometer. In particular, when going on a straight road, the deviation of the GPS/INS system using the dual-antenna GPS is much smaller (less than 3 meters after 15 seconds of signal loss) compared to the case of using magnetic measurement to estimate the yaw angle (more than 10 meters after 15 seconds).

CONCLUSIONS

This paper presented a method to enhance the accuracy and effectiveness of the GPS/INS integrated navigation system using the dual-antenna GPS with the real-time kinematic method. The use of the GPS-RTK method with the dual-antenna GPS resulted in an estimation of the yaw angle that was no longer influenced by the Earth's magnetic field and other external magnetic disturbances. Furthermore, the accuracy of the yaw angle estimation was found to be high, and its accuracy was higher when the baseline distance was greater. Using dual-frequency (L1 and L2) for the GPS produced better results (higher average Fix rate and smaller RMS error) compared to a system that only used the L1 frequency.

We modified the loosely coupled GPS/INS system with yaw estimation from the dual-antenna GPS. The combined system has better performance than the original, particularly in cases where the GPS signal was lost. The experimental results indicated that the system could maintain a position deviation of fewer than 10 meters after a 15-second GPS signal loss.

Currently, the system proposed in this paper still has some limitations. It can only provide good estimations in the case of vehicles moving at low speeds. When the speed increases, the error can increase significantly due to the error of time synchronization between the receivers or between the GPS receiver and the INS system. In the future, the authors will study and evaluate the factors related to synchronization between systems and develop a new system for high-speed autonomous vehicles.

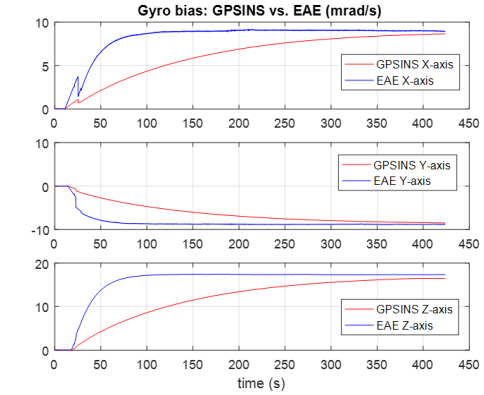

Figure 9: **Gyroscope biases of GPS/INS compared to the Euler angle estimator**.

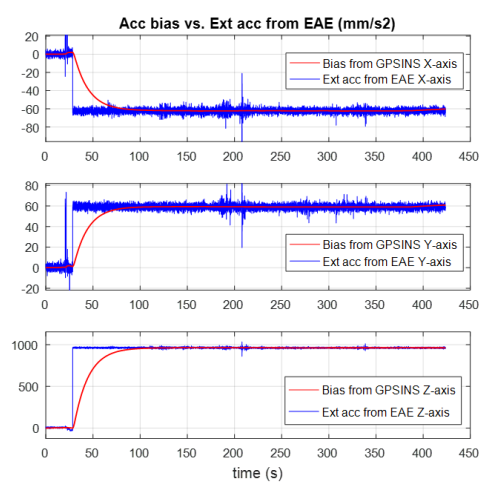

Figure 10: **Accelerometer biases of GPS/INS compared to the Euler angle estimator**.

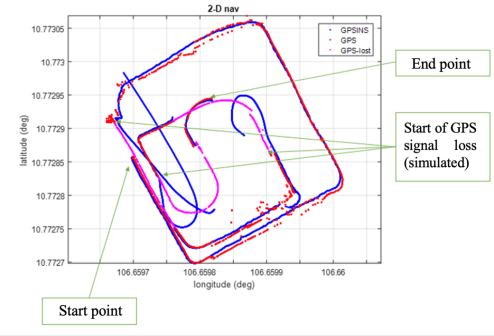

Figure 11: **Experimental result of GPS/INS in the case of using dual-antenna GPS for yaw angle estimation**.

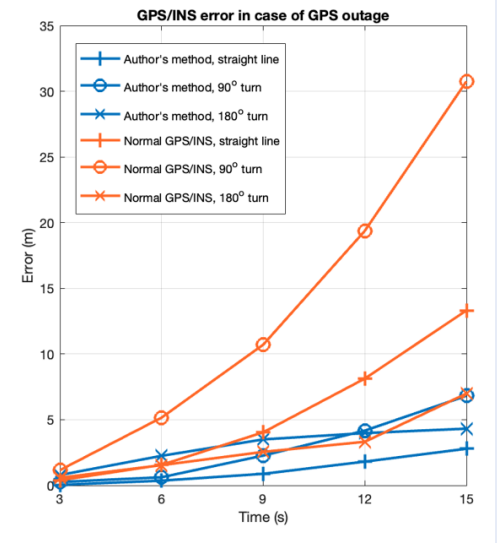

Figure 12: **Error-time graph of the GPS/INS systems when there is a GPS outage**.

LIST OF ABBREVIATIONS AND SYMBOLS

GPS: Global Positioning System
IMU: Inertial Measurement Unit
INS: Inertial Navigation System
LAMBDA: Least squares ambiguity decorrelation adjustment
MLAMBDA: Modified LAMBDA
RTK: Real-Time Kinematic
$[\lambda\ \varphi\ h]^T$: position (longitude, latitude, height)
$v = [v_N\ v_E\ v_D]^T$: velocity (north, east, down)
ϕ, θ, ψ: Euler angles (roll, pitch, yaw)
C_b^n : Direction Cosine Matrix
S_α, C_α : sine and cosine of α
b_a, b_g: accelerometer bias and gyroscope bias

ACKNOWLEDGMENT

This research is funded by the Murata Science Foundation under grant number 22VH07. The authors acknowledge Ho Chi Minh City University of Technology (HCMUT) – VNUHCM for supporting this study.

COMPETING INTERESTS

The authors declare that they have no competing interests.

AUTHOR CONTRIBUTION

Dung Quoc-Tien Tran conducted the research, implemented the model, performed the experiments, and wrote the manuscript. **Vinh-Hao Nguyen** proposed ideas, analyzed the results, and revised the manuscript.

REFERENCES

1. Schmidt GT, Phillips RE. INS/GPS integration architectures;.
2. Ma DM, Shiau JK, Wang IC, Lin YH. Attitude determination using a MEMS-based flight information measurement unit. Sensors (Basel). 2012;12(1):1-23;PMID: 22368455. Available from: https://doi.org/10.3390/s120100001.
3. Eun-Hwan S. Accuracy improvement of low-cost INS/GPS for land applications. The University of Calgary; 2001;.
4. Angrisano A. GNSS/INS integration methods; 2010;.
5. Alatise MB, Hancke GP. Pose estimation of a Moblie robot based on fusion of IMU data and vision data using an extended Kalman filter. Sensors (Basel). 2017;17(10):2164;PMID: 28934102. Available from: https://doi.org/10.3390/s17102164.
6. Al-Sharman MK, Zweiri Y, Jaradat MAK, Al-Husari R, Gan D, Seneviratne LD. Deep-learning-based neural network training for state estimation enhancement: application to attitude estimation. IEEE Trans Instrum Meas. 2020;69(1):24-34;Available from: https://doi.org/10.1109/TIM.2019.2895495.
7. Liu Y, Luo Q, Zhou Y. Deep learning-enabled fusion to bridge GPS outages for INS/GPS integrated navigation. IEEE Sens J. 2022;22(9):8974-85;Available from: https://doi.org/10.1109/JSEN.2022.3155166.
8. Wei X, Li J, Feng K, Zhang D, Li P, Zhao L et al. A mixed optimization method based on adaptive Kalman filter and wavelet neural network for INS/GPS during GPS outages. IEEE Access. 2021;9:47875-86;Available from: https://doi.org/10.1109/ACCESS.2021.3068744.
9. Strohmeier M, Montenegro S. Coupled GPS/MEMS IMU attitude determination of small UAVs with COTS. Electronics. 2017;6(1):15;Available from: https://doi.org/10.3390/electronics6010015.
10. Consoli A, Ayadi J, Bianchi G, Pluchino S, Piazza F, Baddour R et al. A multi-antenna approach for UAV's attitude determination. IEEE metrology for aerospace (metroaerospace), Benevento, Italy, 2015;Available from: https://doi.org/10.1109/MetroAeroSpace.2015.7180690.
11. Nadarajah N, Teunissen PJG, Raziq N. Instantaneous GPS-Galileo attitude determination: single-frequency performance in satellite-deprived environments. IEEE Trans Veh

Technol. 2013;62(7):2963-76;Available from: https://doi.org/10.1109/TVT.2013.2256153.
12. Henkel P, Guenther C. 'Attitude determination with low-cost GPS/INS,' The 26th ION GNSS. Nashville, TN; 2013;.
13. Eling C, Klingbeil L, Kuhlmann H. Real-time single-frequency GPS/MEMS-IMU attitude determination of lightweight UAVs. Sensors (Basel). 2015;15(10):26212-35;PMID: 26501281. Available from: https://doi.org/10.3390/s151026212.
14. Takasu T. RTKLIB ver 2.4.2 Manual, 2013;.
15. Chang X-W, Yang X, Zhou T. MLAMBDA: a modified Lambda method for integer least-squares estimation. Geodesy. 2005;79(9):552-65;Available from: https://doi.org/10.1007/s00190-005-0004-x.
16. Petovello M. Real-time integration of a tactical-grade IMU and GPS for high-accuracy positioning and navigation. Canada: University of Calgary; 2003;.
17. U-blox AG. Ublox NEO-M8P datasheet [online];Available from: https://content.u-blox.com/sites/default/files/NEO-M8P_DataSheet_UBX-15016656.pdf.
18. NovAtel. OEMV-2 product sheet [online];Available from: https://hexagondownloads.blob.core.windows.net/public/Novatel/assets/Documents/Papers/OEMV2/OEMV2.pdf.